Hindawi Publishing Corporation
Journal of Nanomaterials
Volume 2012, Article ID 302046, 12 pages
doi:10.1155/2012/302046

Research Article

Layer-by-Layer Self-Assembled Metal-Ion- (Ag-, Co-, Ni-, and Pd-) Doped TiO_2 Nanoparticles: Synthesis, Characterisation, and Visible Light Degradation of Rhodamine B

Mphilisi M. Mahlambi,[1] Ajay K. Mishra,[1] Shivani B. Mishra,[1] Ashok M. Raichur,[1,2] Bhekie B. Mamba,[1] and Rui W. Krause[1]

[1] *Department of Applied Chemistry, University of Johannesburg, P.O. Box 17011, Doornfontein 2028, South Africa*
[2] *Department of Materials Engineering, Indian Institute of Science, Bangalore 560012, India*

Correspondence should be addressed to Ashok M. Raichur, amr@materials.iisc.ernet.in

Received 25 January 2012; Revised 13 March 2012; Accepted 13 March 2012

Academic Editor: Grégory Guisbiers

Metal-ion- (Ag, Co, Ni and Pd) doped titania nanocatalysts were successfully deposited on glass slides by layer-by-layer (LbL) self-assembly technique using a poly(styrene sulfonate sodium salt) (PSS) and poly(allylamine hydrochloride) (PAH) polyelectrolyte system. Solid diffuse reflectance (SDR) studies showed a linear increase in absorbance at 416 nm with increase in the number of m-TiO_2 thin films. The LbL assembled thin films were tested for their photocatalytic activity through the degradation of Rhodamine B under visible-light illumination. From the scanning electron microscope (SEM), the thin films had a porous morphology and the atomic force microscope (AFM) studies showed "rough" surfaces. The porous and rough surface morphology resulted in high surface areas hence the high photocatalytic degradation (up to 97% over a 6.5 h irradiation period) using visible-light observed. Increasing the number of multilayers deposited on the glass slides resulted in increased film thickness and an increased rate of photodegradation due to increase in the availability of more nanocatalysts (more sites for photodegradation). The LbL assembled thin films had strong adhesion properties which made them highly stable thus displaying the same efficiencies after five (5) reusability cycles.

1. Introduction

Photocatalytic reaction-based processes are becoming more attractive to industry because they provide an alternative avenue for the decomposition of environmental pollutants. Growth in industrial development can be directly linked to the emergence of toxic pollutants which are deposited into aqueous streams [1, 2]. Among the semiconductor catalysts, TiO_2 (titanium dioxide or titania) is close to the ideal benchmark in environmental photocatalytic applications because of its outstanding chemical and biological stability, abundance, high oxidative power and, it is comparably less expensive [3–9].

Although the use of TiO_2 in suspension form is more feasible due to its large surface area, there are four major technical challenges that restrict large-scale application of titania. Firstly, it has a relatively wide band gap (~3.2 eV, which falls in the UV range of the solar spectrum); therefore, it has minimal absorption of visible light and is unable to harness visible light hence ruling out sunlight as the energy source of photoactivation [7, 8, 10–14]. Secondly, it has low quantum efficiency due to the low rate of electron transfer to oxygen resulting in a high recombination of the photo generated electron-hole pairs [5, 7, 10]. Therefore, the effective utilisation of visible light for photocatalytic processes has become the ultimate goal. To achieve this, various methods like substitutional doping (N.C, F, etc.), dye sensitizing, using narrow band-gap quantum dots, binary oxides, and noble and transition metal nanoparticles have been developed [15, 16]. Also, the photoactivity of TiO_2 nanoparticles has been tailored by exposing the {001} facets which are very active [17]. Although these facets are very

active, they easily diminish crystal during nucleation and growth due to that they possess a high surface [17, 18]. Doping metals into the TiO_2 lattice is an effective strategy to reduce the band gap and shift the absorption edge towards visible-light region as they create energy states within the band gap by providing a "cushion" on the valence band (the donor level), resulting in a "decrease" in the band gap and also by acting as electron scavengers hence resulting in increased photocatalysis [7, 19–25]. However, it is imperative to take into consideration the amount of the dopant (metal) when preparing doped titania because when the dopant level surpasses the optimal limit, which usually lies at a very low dopant concentration (~0.4%), the metal ions act as recombination centres resulting in reduced photoactivity [23, 26]. Thirdly, when used in a suspension, titanium dioxide aggregates rapidly due to its small size (4–30 nm) suspended particles may scatter the light beam thus reducing its catalytic efficiency [8, 27, 28]. Lastly, the application of powdered TiO_2 catalysts requires posttreatment separation to recover the catalyst which is normally difficult, energy consuming, and economically not viable [1, 5, 8, 27, 29].

These technical challenges have led to more research activities on the fabrication of different types of titania thin films [6, 8, 9, 30–33]. Generally, thin films are known to be chemically stable and possess a high dielectric constant, a high refractive index, and excellent transmittance [9]. The most common methods for synthesising thin films include among others chemical vapour deposition (CVD), spray pyrolysis, dip coating, spin coating, liquid-phase deposition (LPD), ion-assisted deposition, arc-ion planting, sputtering, and sol-gel [11, 19, 32, 34–39]. However, these methods have some drawbacks. For example, although the sol-gel technique is the most widely used method, its disadvantage is the difficulty to control film thickness. The CVD method requires high temperatures while cracking and peeling off of the catalyst layer is usually observed due to poor adherence of the photocatalyst on the support [1, 8], and LPD requires special raw materials [38], hence they are not suitable for industrial applications.

In our laboratories we have used an alternative thin film synthesis method, layer-by-layer (LbL) self-assembly technique, to synthesise TiO_2 thin films of high quality [1]. The LbL technique can be used to deposit different types of materials on various substrates with good control of the thickness of the materials deposited on the substrate at nanometer-scale precision [1, 40–42]. The technique allows for alternate layer-by-layer growth of films through adsorption of polycation and polyanion monolayers from their aqueous solutions. The ionic attraction between opposite charges is the driving force for the multilayer buildup [40, 43–45]. This approach has been found to be a more economic alternative method compared to other methods for the direct preparation of thin films because it is simple, cheap, deposition occurs at low temperatures (room temperature), ease of control of film thickness (from nanometers to micrometers), and does not require complex equipment to execute [42, 44, 46, 47].

Layer-by-layer synthesised thin films have found applications, in a variety of scientific applications, and these include biosensors, controlled drug delivery, surface coatings, and environmental applications in the degradation of toxic pollutants [8, 44, 48–52]. TiO_2 nanoparticles have also been successfully assembled on substrates using electrolytic polymers resulting in improved photocatalytic performances [1, 36, 53, 54]. These photocatalytic processes were performed under UV irradiation. However, most research activities in semiconductor photocatalysis focus on the development of a system that employs natural solar energy to degrade toxic pollutants in an aqueous medium. To achieve this, we have synthesised metal-ion- (Ag-, Co-, Ni-, and Pd-) doped titania thin films through the LbL self-assembly technique. Pd is highly reactive, and Ni is almost the same size as Ti. Pd and Ni are also abundant in South Africa hence are readily available and inexpensive. Ag and Co were used for comparative purposes. Metal-ion-doped TiO_2 (m-TiO_2) thin films have been previously synthesised using either sol-gel, liquid-phase deposition or colloidal sol techniques [5, 7, 10, 19, 28] but not using the layer-by-layer self-assembly deposition. To the best of our knowledge, the application of the LbL technique and the polyelectrolyte system used to immobilise the catalysts as described in this study has not been reported in the literature.

The photocatalytic efficiencies of these metal-ion-doped titania thin films were determined by the degradation of Rhodamine B, a xanthene group dye, under visible light. Rhodamine B (Rh B) was chosen because it is one of the major pollutants found in the textile and photographic industry effluents [55, 56]. Furthermore, it is estimated that approximately 1 to 20% of the total world produce of dyes is lost to the environment during synthesis and dyeing processes. These textile effluents are an environmental burden as they contain large amounts of azoic, anthraquinonic, and heteropolyaromatic dyes [55]. The discharge of these highly pigmented synthetic dyes to the ecosystem causes aesthetic pollution, eutrophication, and perturbations of aquatic life. Therefore, in this study we have used Rhodamine B as a model pollutant.

In this paper, we report on the photodegradation of Rhodamine B by poly(styrene sulfonate/metal-ion-doped titania (PSS/m-TiO_2)) multilayer thin films. The presence of the metals on the titania lattice shifts the absorption edge of titania to the visible-light region while the thin films eliminate the problems of suspension aggregation and posttreatment. The value-add of this work is the development of a system that can be potentially used in daylight to degrade pollutants in an aqueous media without leaving residual nanoparticles in the treated media. Poly(styrene sulfonate) was chosen because it is a strong polyelectrolyte that is negatively charged at all pH values. To study the cost effectiveness and sustainability of the prepared thin films, catalyst reusability studies were also performed.

2. Experimental

2.1. Materials and Methods. A Model Orion 5 star digital pH (Thermo Electron Corporation, USA) was used for determining the pH of the solutions. HCl or NaOH (1 M)

was used to adjust the pH of the prepared solutions. Microscopic glass slides (25.4 × 63.5 mm) were used as catalyst substrates. Poly(styrene sulfonate) (PSS, M_W = 70 000 g/mol) and poly(allylamine hydrochloride) (PAH, M_W = 70 000 g/mol) were purchased from Sigma-Aldrich (USA). Metal-ion-doped TiO_2 nanoparticles were synthesised by modifying a sol-gel method reported by Zhu et al. [57]. Titanium (IV), tetraisopropoxide (TTIP) (99%), and $NiNO_3$ were bought from Sigma-Aldrich (Germany) and used without further purification. Formic acid (98%) was purchased at Merck, and AR grade *n*-propanol was sourced from SD's Fine Chemicals (Pty) Ltd. and was distilled before usage. $PdCl_2$ and Rhodamine B were supplied by Finar Chemicals (Mumbai, India), $AgNO_3$ was procured from Associated Chemicals Enterprises (Pty) Ltd., whereas $Co(NO_3)_2$ was sourced from Hopkins and Williams Ltd., Essex, UK.

2.1.1. Synthesis of Catalysts. Titanium (IV) tetraisopropoxide (10 mL, 0.334 mol) was dissolved in propanol (48 mL, 0.642 mol), and the reaction mixture was stirred for 20 min. The metal salt $AgNO_3$ (0.4%) was dissolved in water (5 mL) while the other salts ($PdCl_2$, $Co(NO_3)_2$, and $NiNO_3$) (0.4%) were dissolved in *n*-propanol (5 mL) and were added dropwise to the reaction mixture of TTIP and propanol. Formic acid (13 mL, 0.535 mol) was gradually added while stirring gently. After stirring the reaction mixture for a further 20 min, a precipitate (metal-ion-doped titanium hydroxide) was gradually formed. The precipitated solution was stirred for a further 2 h period, aged at room temperature for another 2 h, and filtered. The filtered residue was then repeatedly washed with copious amounts of propanol and deionised water; thereafter, it was dried overnight in an oven at 80°C. The precipitate was then ground into fine powder using a mortar and pestle and then calcined at 450°C for 6 hrs at a heating rate of $2°\text{min}^{-1}$ to obtain nanosized metal ion-doped TiO_2 photocatalysts. All experiments were carried out at room temperature.

2.1.2. LbL Thin Film Synthesis. The thin films were immobilised on glass slides using the method described by Decher et al. [41]. The glass slides were cleaned by first sonicating for 10 min in a 2 : 1 (v/v) ratio of isopropanol and water followed by rinsing with deionised water. Poly(allylamine hydrochloride), and poly(styrene sulfonate) solutions ($1\,\text{g L}^{-1}$) were prepared using deionised water, and the pH of the solutions was adjusted to 2.5. The pH of the water used for rinsing was also adjusted to the same pH. A metal-ion-doped TiO_2 colloidal suspension was made in deionised water, and its pH was adjusted to that of the electrolyte solutions for the deposition of the thin films by the LbL technique. Polyelectrolyte solutions (PELs, $100\,\text{mg L}^{-1}$) and metal-ion-doped TiO_2 colloidal suspensions of $4\,\text{g L}^{-1}$ concentration, that is, 0.4% wt were prepared in deionised water and deposited on both sides of the glass slides. Based on the isoelectric point of TiO_2 (6.6), TiO_2 is positive and stable at pH 2.5, and PSS is negative at all pH values while PAH is positive below pH = 4. Before deposition of the films on the substrates, the charge (on the substrates) was reversed (positive) by the deposition of a PAH monolayer. Thereafter, alternate layers of PSS and m-TiO_2 were deposited with m-TiO_2 being the last layer to be deposited in all instances.

2.2. Characterisation

2.2.1. UV-Visible Diffuse Reflectance Spectroscopy. The absorbance spectra of the prepared PSS/m-TiO_2 were obtained from a T60U spectrophotometer (PG Instruments Ltd., London, UK) and were recorded from 600 nm to 300 nm range. Since the film deposition was on both sides of the slide, the absorbance reported is also for the two sides of the glass slide.

2.2.2. SEM and EDX Analysis. A field emission microscope (FEI SIRION SEM, Eindhoven, The Netherlands) was used to analyse and visualise the quality and morphology of the synthesised thin films. The extent of LbL thin film deposition was also studied by the scanning electron microscope. The thin films were coated with gold prior to analysis. The SEM was coupled with an EDX detector in order to confirm the elemental composition of the thin films.

2.2.3. AFM Analysis. A Nanosurf EasyScan 2 (Switzerland), atomic force microscope (AFM) was employed to view the topography of the thin films. The AFM was also used to verify the effectiveness of the LbL technique on the deposition of thin films. The AFM was operated in the contact mode with the cantilever being in contact with the thin film surface.

2.3. Visible-Light Degradation Studies

2.3.1. Visible-Light Degradation. The ability of the thin films to degrade Rhodamine B under visible light was studied using a high-pressure powerball HCI-T 70W/NDL mercury vapour lamp with a maximum wavelength range of 410–460 nm (Osram, Germany). The photocatalytic degradation experiments were carried out in a photoreactor chamber. The photoreactor was set up and enclosed in a wooden box. It had a jacketed quartz tube with dimensions of 3.4 cm (inner diameter), 4 cm (outer diameter), and 21 cm (length). A submersible water pump was used to propel and circulate water through the quartz tube to avoid heating up of the photodegradation chamber due to the visible-light irradiation. The immobilised catalysts were placed in the dye solution, and the solution was continuously stirred with a magnetic stirrer. The stirring ensured a continuous flow of the solution over the catalysts during the photocatalytic experiments and hence promote the degradation process.

2.3.2. UV-Vis (Quantification) and Kinetics. The photocatalytic activity of the PSS/m-TiO_2 nanophotocatalysts was studied using Rhodamine B dye (100 mL, $10\,\text{mg L}^{-1}$). The red dye was poured into a beaker, placed in the photoreactor, and the solution was stirred using a magnetic stirrer for 30 min prior to irradiation with visible light to obtain a catalyst/dye adsorption-desorption equilibrium. Aliquots of

2 mL were extracted from the reaction chamber at 30 min intervals for 6.5 h to measure the extent of the degradation.

The kinetics of the photodegradation process was studied using the apparent rate constant. The apparent rate constant allows for the determination of photocatalytic activity independent of the previous adsorption period and the concentration of the Rh B remaining in the solution [58]. The data was fitted into the first order kinetic equation. The apparent first order kinetic equation is $-\ln(C_t/C_0) = K_{app}t$, where K_{app} is the apparent rate constant, C_t, the solution phase concentration, and C_0, the concentration at $t = 0$, and it was used to fit the experimental data [26].

2.3.3. Catalyst Reusability. The importance of catalyst reusability is important when considering cost and economic implications. To study the reusability of the m-TiO_2 thin films, the degraded dye solution was removed after the first cycle, without removing the catalyst. A fresh solution of the dye was poured into the beaker, and the irradiation was started. This procedure was repeated over five (5) cycles for 6.5 h, and the solution was analysed after each cycle to determine the extent of degradation by the recycled catalysts.

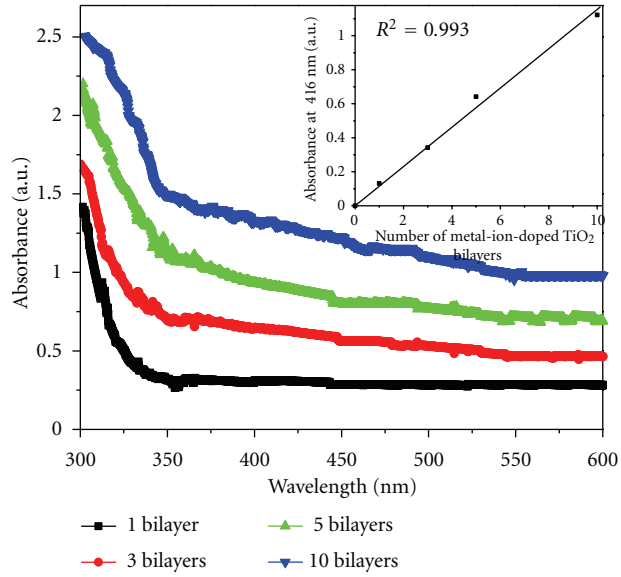

FIGURE 1: Absorption spectra of PSS/m-TiO_2 showing increase in absorbance with increase in number of layers (0.4% wt%). Insert: number of PSS/m-TiO_2 versus absorbance.

3. Results and Discussions

3.1. UV-Visible Diffuse Reflectance Spectroscopy. Figure 1 shows the UV-Visible solid diffuse reflectance (SDR) spectra of the thin films. For the SDR measurements, 1, 3, 5, and 10 m-TiO_2 layers were each deposited on glass slides. Poly(allylamine hydrochloride) was the initial layer followed by alternate layers of PSS and m-TiO_2, respectively. Glass absorbs UV light, but it gives specious peaks below 300 nm, thus, a wavelength of 300 nm to 600 nm was chosen. The maximum UV absorbance of metal-ion-doped titania is 416 nm [59], and PSS has a characteristic absorption peaks at 220 nm while PAH shows negligible absorbance under the UV-vis region [1]. Hence, the absorption spectra recorded were characteristic of only m-TiO_2. From Figure 1 it can be seen that as the number of the deposited bilayers increased the absorbance also increased [1, 47, 53]. Also, the insert graph further reveals that the absorbance increased linearly as the number of metal-ion-doped titania bi-layers were increased.

3.2. SEM and EDX Analysis. The SEM micrographs of the synthesised thin films (1 to 5 bi-layers) in Figure 2 demonstrate that as the number of depositions of the thin films increased, there was also an increase in the metal-ion-doped titania nanoparticles assembled on the glass substrates. This observation can also be used to explain the increase in the absorbance noted in the UV-Vis spectroscopy. Furthermore, as the number of the deposited bilayers was increased from 1 to 10, the thin films assumed a more uniform distribution of the nanoparticles, a special trend exhibited by layer-by-layer self-assembled thin films [60]. Furthermore, SEM characterisation showed a smooth surface morphology as a result of a network of crosslinked polyelectrolytes, and m-TiO_2 nanoparticles [61]. Also, a high degree of porosity of the thin films was observed on the SEM micrographs, and this property plays an important role in the photocatalytic activity of the assembled m-TiO_2 nanoparticles [1, 53]. The porosity nature of the thin films confirms the presence of a large surface area which results in an increased photocatalytic activity.

Electron dispersive X-ray spectroscopy (Figure 3) provided evidence of the successful synthesis of the metal-ion-doped titania thin films. The presence of the metal ions (Ag, Co, Ni, and Pd) is further indication that doped metal ions formed part of the titania lattice. The Si and Ca peaks observed from the EDX spectra of the thin films emanate from the glass slides used as the substrate used for assembling the metal-ion-doped titania nanoparticles [62].

3.3. AFM Analysis. The AFM images revealed an increase in surface coverage of metal-ion-doped titania nanoparticles as the number of the deposited bi-layers increased from 1 to 10. Also, the topography of the thin films showed patches and gaps between the nanocatalysts which became smaller and eventually became closely packed as the number of bi-layers increased. This is as a result of the overlap of the nanocatalyst layers forming a network as they adhere to oppositely charged surfaces (self-assembly) due to the presence of free charges from the previous depositions [40]. Also, from the 3D AFM images there seems to be an increased roughness of the thin film topography as the number of the bi-layers increased [63]. This suggests that the thin films had an increased surface area which is desirable for increased photocatalytic activity.

Furthermore, the AFM images confirm that there is an increase in film thickness as the number of deposited layers is increased (Figure 4). The linear fit (Figure 5) had a regression value of 0.994 which indicates a uniform growth

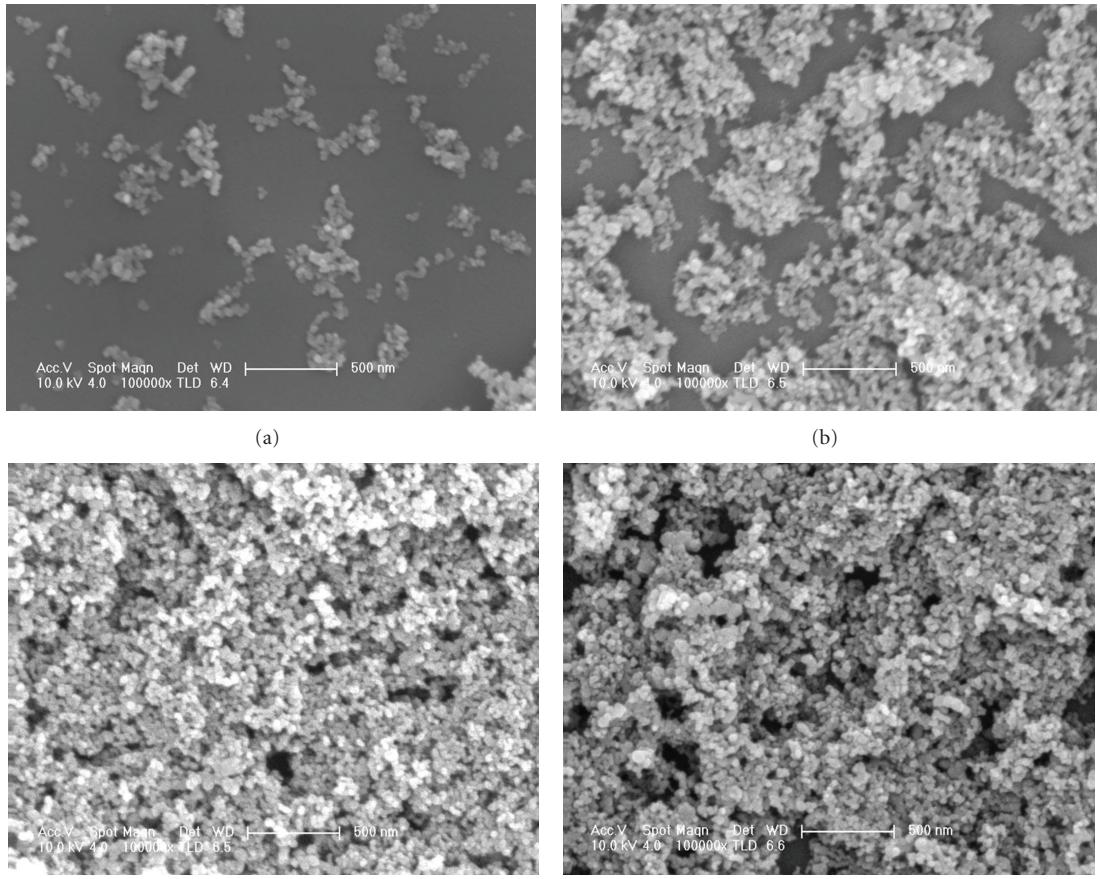

FIGURE 2: SEM images of $(PSS/m\text{-}TiO_2)_n$, where n = number of deposited layers, 1 (a), 3 (b), 5 (c), and 10 (d) immobilised on glass slides by LbL self-assembly technique.

of the PSS/TiO_2 thin films. The average thickness of the m-TiO_2 thin films was estimated to be 19.2 nm. Generally, the thickness of PSS/TiO_2 bi-layer thin films is estimated to be approximately 19 nm [1]. Film thickness is largely dependent on the polyelectrolyte used, the pH during deposition, and the size of the nanoparticles deposited because this is directly related to the amount of TiO_2 deposited on the substrate. For example, a single bi-layer of PAA/TiO_2 and $PDAC/TiO_2$ thin films is estimated to be around 18 nm and 38 nm, respectively [1, 64]. Since one (1) bi-layer of PSS/TiO_2 is estimated to be 19 nm, theoretically PSS/TiO_2 thin films having three (3) and ten (10) bi-layers are expected to be 57 nm and 190 nm thick, respectively, hence the values of 58.3 nm and 186 nm obtained for the synthesised $PSS/m\text{-}TiO_2$ thin films compare favourably to the reported values.

3.4. Visible Light Degradation of Rhodamine B and Kinetic Studies. The photodegradation process of Rhodamine B can be summarised in (1) to (3) when disregarding the role of the electrons (e^-) which is in the oxidation of metal ions. The titania nanocatalysts absorb a photon ($h\nu$) resulting in the excitation of an electron (e^-) from the valence band (VB) to the conduction band (CB) leaving an electron vacancy or a hole (h^+) in the valence band (1). The holes then migrate to the surface of the titania where they react with surface hydroxyl groups in the TiO_2 lattice or water to produce hydroxyl radicals (2).

$$\text{m-TiO}_2 + h\nu \longrightarrow \text{h}^+ + \text{e}^-, \tag{1}$$

$$\text{h}^+ + \text{m-TiO}_2 \longrightarrow \text{m-TiO}_2 + {}^\bullet\text{OH}, \tag{2}$$

$${}^\bullet\text{OH} + \text{RhB} \longrightarrow \text{Degraded products}. \tag{3}$$

The hydroxyl radicals then react with the Rhodamine B producing intermediates, carbon dioxide, water, and inorganic ions (3).

UV-visible spectroscopy was used to quantify the amount of Rhodamine B photodegraded by the $m\text{-}TiO_2$ layer-by-layer thin films assembled on glass slides. Glass slides with different thin film thicknesses, that is, 1 to 10 bi-layers were investigated for the photodegradation of Rhodamine B. Five immobilised catalysts (i.e., 5 glass slides) of each bi-layer sequence were put in Rhodamine B solution (100 mL of 100 mg L^{-1}) and stirred for 30 min in the dark to attain an adsorption-desorption equilibrium between the

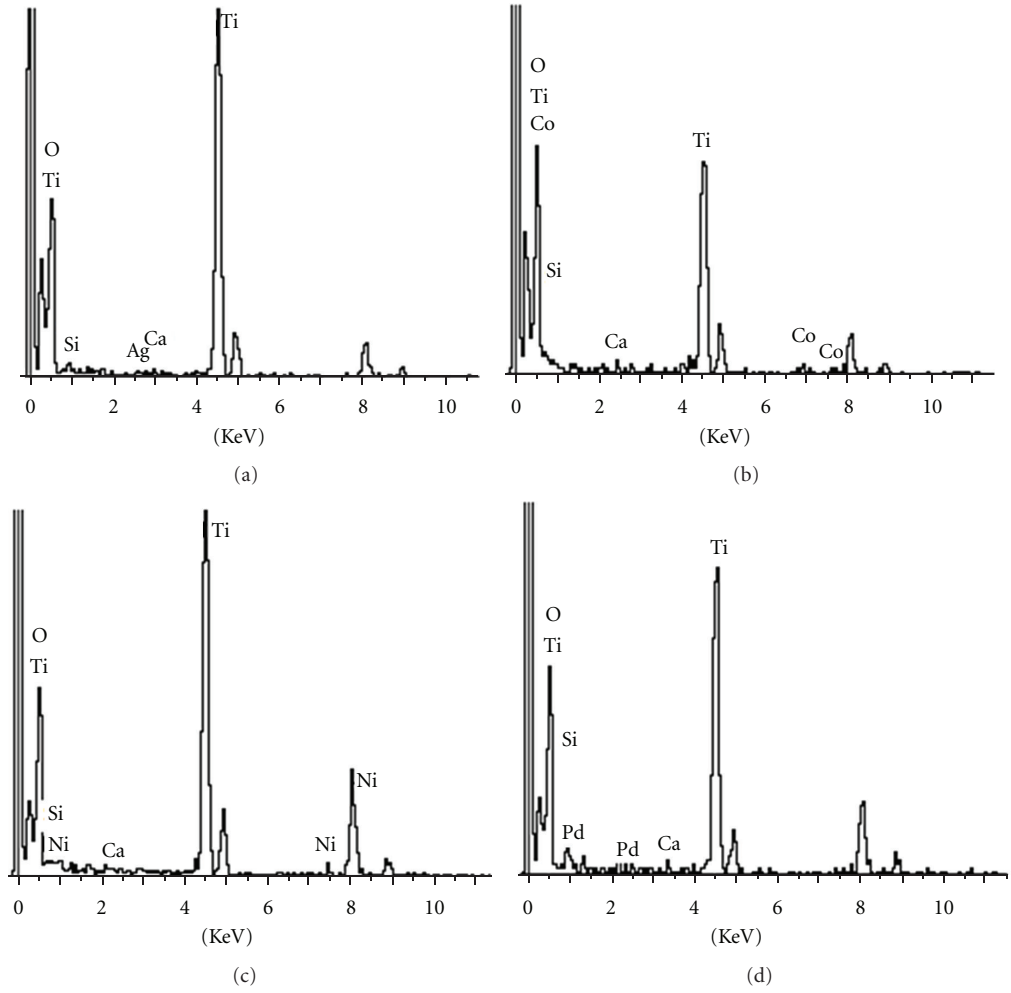

Figure 3: EDX spectra of $(PSS/m\text{-}TiO_2)_{10}$ for Ag-, Co-, Ni-, and Pd-, doped titania immobilised on glass slides by LbL self-assembly technique.

catalyst and the Rhodamine B. The reaction mixture was then illuminated for 6.5 h, and 2 mL aliquots of the dye were taken to study the extent of the photodegradation. Visible-light illumination without the semiconductor catalyst produced no photodegradation of the dye without. Poly(styrene sulfonate) and PAH do not take part in the photodegradation of Rhodamine B by TiO_2 nanoparticles [1]. The photodegradation kinetic studies were studied using the first order apparent rate law equation ($-\ln C_t/C_0 = K_{app}t$).

3.4.1. Ag-TiO_2 Thin Films. The photodegradation experiments showed that 5 of catalysts 1 bi-layer degraded 33%, 3 bi-layers had degraded 48%, 5 bi-layers had degraded 79%, and 10 bi-layers had degraded 96% of Rhodamine B after 6.5 h of visible-light irradiation (Figure 6). These results confirm that as the number of bi-layers is increased, there is also an increase in the rate of photocatalytic degradation of Rhodamine B. Further confirmation can be drawn from the apparent rate constants obtained from the linear transform graph. As the number of bi-layers increased from 1 to 10, the apparent rate constant also increased from 0.0012 min^{-1} to 0.0102 min^{-1} as shown in Table 1.

3.4.2. Co-TiO_2 Thin Films. For the Co-TiO_2 immobilised thin films, photodegradation efficiencies of 33%, 51%, 76%, and 97% were observed for 1, 3, 5, and 10 bi-layers after 6.5 h of visible-light irradiation. Increasing the number of bi-layers resulted in an increase in the rate of photocatalytic degradation of Rhodamine B. The apparent rate constants observed for these photocatalytic degradation efficiencies were 0.0012 min^{-1} for a single bi-layer, 0.0022 min^{-1} for 3 bi-layers, 0.0043 min^{-1} for 5 bi-layers, and 0.0102 min^{-1} for 10 bi-layers.

3.4.3. Ni-TiO_2 Thin Films. The same photodegradation trend was observed for Ni-TiO_2 LbL assembled thin films. After 6.5 h of visible-light irradiation, it was observed that 1 bi-layer of the Ni-titania film has degraded only 3.5 mg L^{-1} (35%), 3 bi-layers had degraded 5.6 mg L^{-1} (56%), and 5 bi-layers had degraded 6.2 mg L^{-1}, an equivalent of 62% of Rhodamine B. The highest photodegradation efficiency

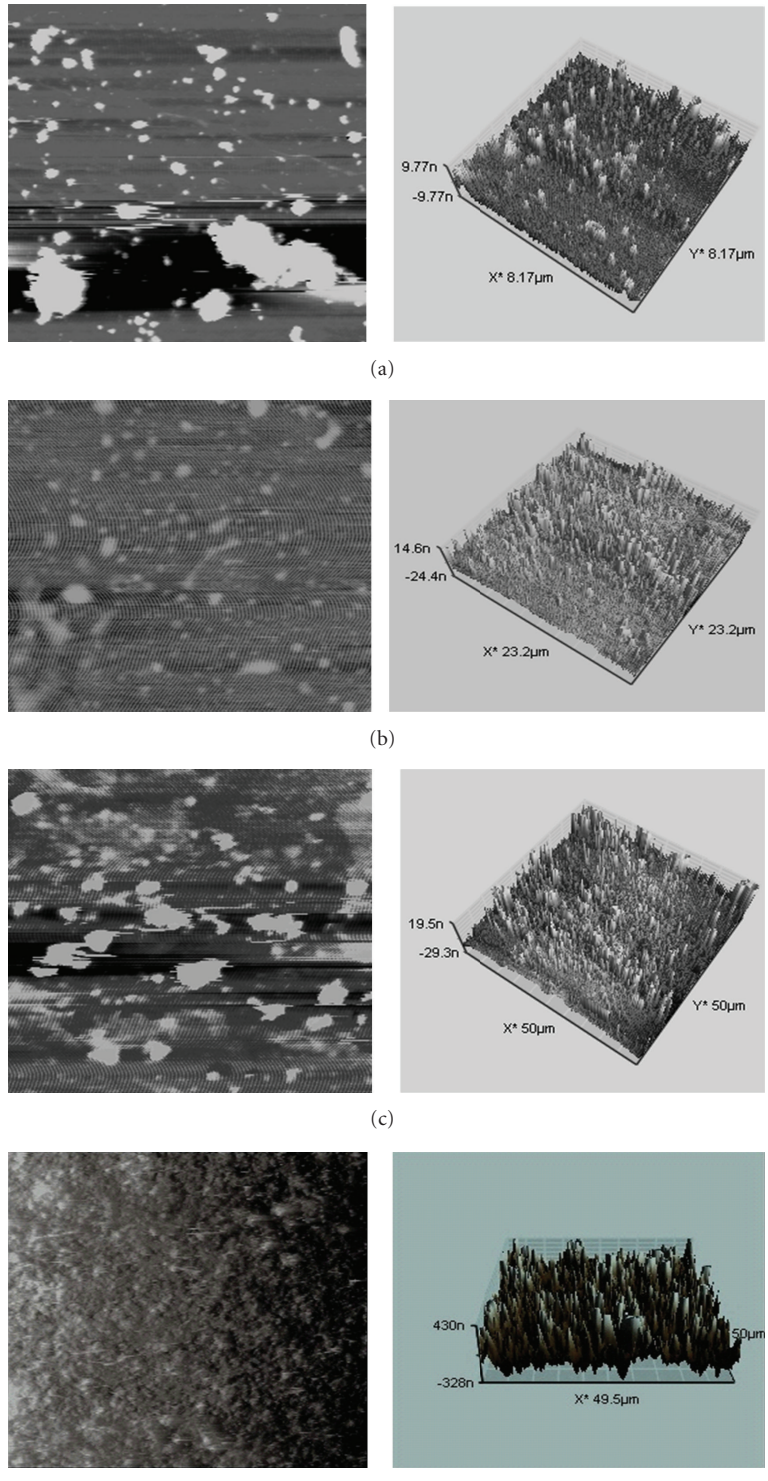

Figure 4: 2D and 3D AFM images of $(PSS/m\text{-}TiO_2)_n$, where $n = 1$ (a), 3 (b), 5 (c), and 10 (d) immobilised on glass slides by LbL self-assembly technique.

was observed for the 10 bi-layers (85%). This confirms that enhancement of the initial rate of photodegradation (apparent rate) of Rhodamine B corresponds to an increase in the number of bi-layers (Table 1).

3.4.4. Pd-TiO_2 Thin Films. The Pd-TiO_2 thin films also produced the same photodegradation pattern that was observed for the Ag-, Co-, and Ni-TiO_2 thin films, that is, there was an increase in the rate of photodegradation

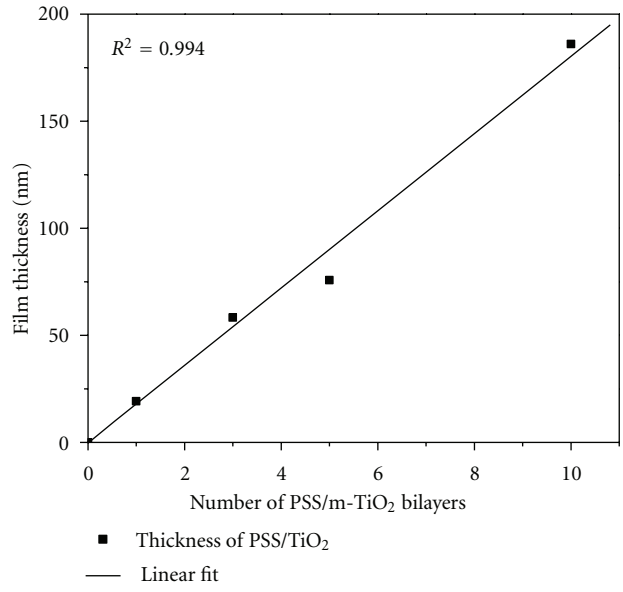

Figure 5: Number of PAH(PSS/m-TiO_2)$_n$ bilayers versus film thickness (n = 1, 3, 5, and 10).

Table 1: Photocatalytic degradation efficiencies and apparent rate constants of the thin films.

Catalyst	No. of bi-layers	Apparent rate constant (min^{-1})	Degradation after 6.5 h (%)
Degussa P25	10	0.0008	20
Ag-TiO_2	1	0.0012	33
	3	0.0019	48
	5	0.0047	79
	10	0.0092	96
Co-TiO_2	1	0.0012	33
	3	0.0022	51
	5	0.0043	76
	10	0.0102	97
Ni-TiO_2	1	0.0013	35
	3	0.0025	56
	5	0.0029	62
	10	0.0059	85
Pd-TiO_2	1	0.0013	35
	3	0.0022	51
	5	0.0029	61
	10	0.0083	94

as the number of bi-layers increased. The photocatalytic efficiencies obtained after 6.5 h of visible-light irradiation increased from 35% to 94% as the number bi-layers increased from 1 to 10, respectively. These efficiencies corresponded to apparent rate constants of 0.0013 min^{-1} and 0.0083 min^{-1}, respectively. The rest of the apparent rate constants and photodegradation efficiencies are shown in Table 1.

The increase in the absorption efficiencies observed with increase in the number of bi-layers is most probably due to increase and availability of more surface area of the catalyst. Furthermore, as the number of bi-layers increase, there was a direct increase in the amount of catalysts embedded on the substrate as shown by the SEM and AFM images. The initial rate, that is, the apparent rate constant of degradation of Rhodamine B was observed to increase with increasing number of bi-layers. This is an indication that the photodegradation is not only affected by the outermost layer but also the inner preceding layers. The participation of the inner layers in the photodegradation is possible due to the high degree of porosity and roughness exhibited by the thin films as shown by the SEM and AFM images, respectively. These resulted in an increased surface area for Rhodamine B adsorption and hence an increased rate of photocatalytic degradation.

To further ascertain the reactivity of the synthesised metal-ion-doped thin film catalysts, their photocatalytic activities were compared with the Degusa P25 titania nanocatalysts. The synthesized thin films were found to be superior to the Degusa P25 thin films which could only degrade up to 20% Rhodamine B under visible-light irradiation over a 6.5 h period (Table 1). Although these Degusa P25 thin films show high degradation efficiencies under UV-light irradiation [1], they fail to possess the same under visible-light. This therefore proves that the presence of the metalions on the titania lattice has played a pivotal role in shifting the absorption edge of the titania nanocatalysts towards visible light. Hence, this study provides a major stride towards the use of solar energy (visible light) for the activation of titania nanoparticles for use in environmental remediation processes.

3.4.5. Effect of Metal-Ion on the Rate of Photodegradation. The results of Rhodamine B photodegradation show average degradation efficiencies of about 33%, 50%, 70%, and 93% for the 5 catalysts of 1, 3, 5, and 10 bi-layers of m-TiO_2 thin films (Figure 7), respectively. These average degradation efficiencies were irrespective of the metal ion used during the 6.5 h of visible-light irradiation. The only metal-ion-doped catalyst that showed lower absorption efficiencies for 10 bi-layer thin films was Ni-TiO_2 titania (shown by the larger error bar on the 10 bi-layer thin films (Figure 7)). This could be as a result of the photocatalytic activity of m-TiO_2 being affected by the slide orientation. Although the incident visible-light intensity was the same for all the experiments, the slides might not have been identically oriented hence the absorption of visible light by the slides might not be the similar. This suggests that the rate of production of radicals was not identical for all the glass slides thus resulting in slight differences in the photodegradation efficiencies.

3.5. Catalyst Reusability. To investigate the catalyst reusability studies, PAH(PSS/m-TiO_2)$_{10}$ (where m = Ag, Co, Ni, or Pd) thin films were used. The catalyst reusability studies were performed over five (5) cycles (Figure 8). The results

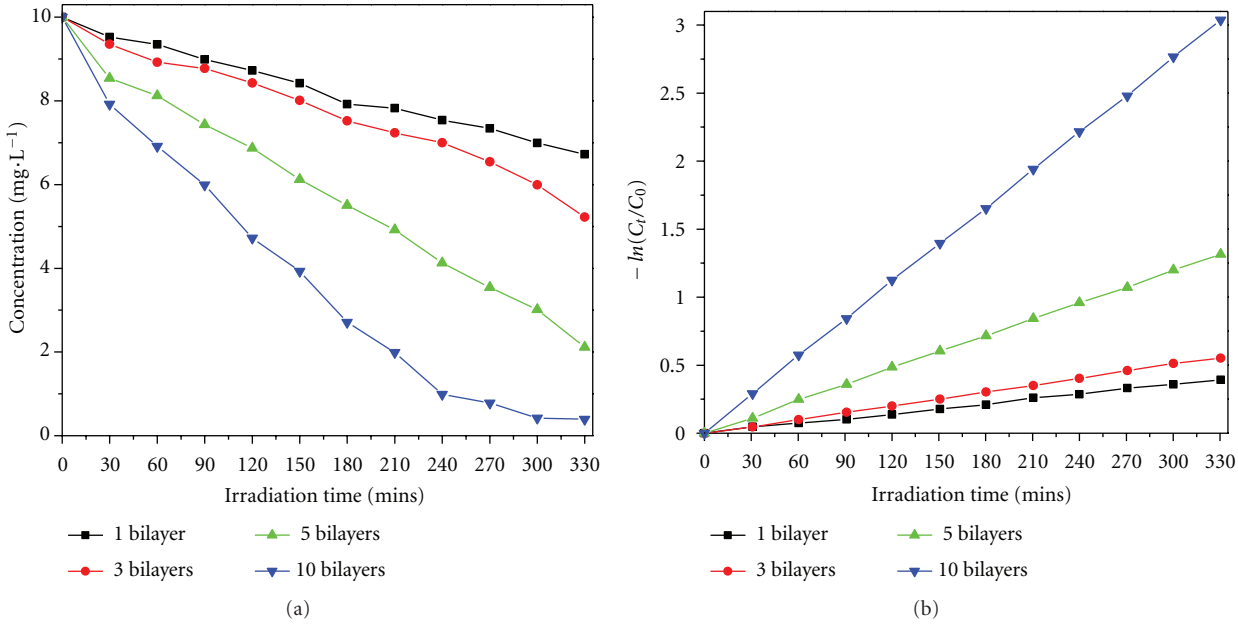

FIGURE 6: Photocatalytic degradation of Rh B and the linear transform, $-\ln(C_t/C_0) = f(t)$, of the kinetic curves of Rh B disappearance by Ag-TiO_2 thin films (1–10 bi-layers).

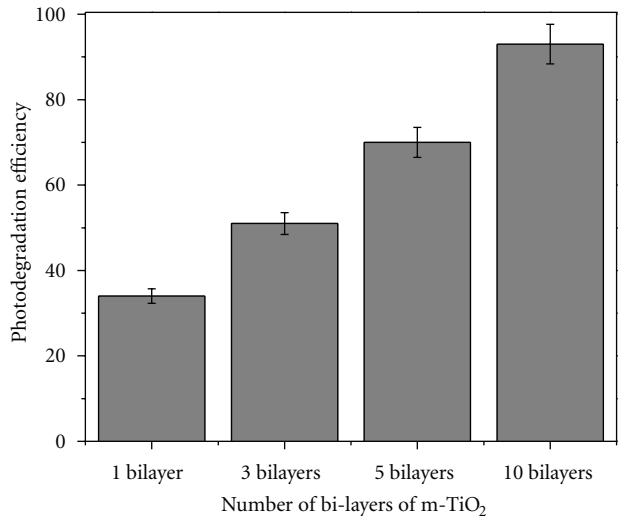

FIGURE 7: Absorption efficiencies exhibited by the m-TiO_2 thin films.

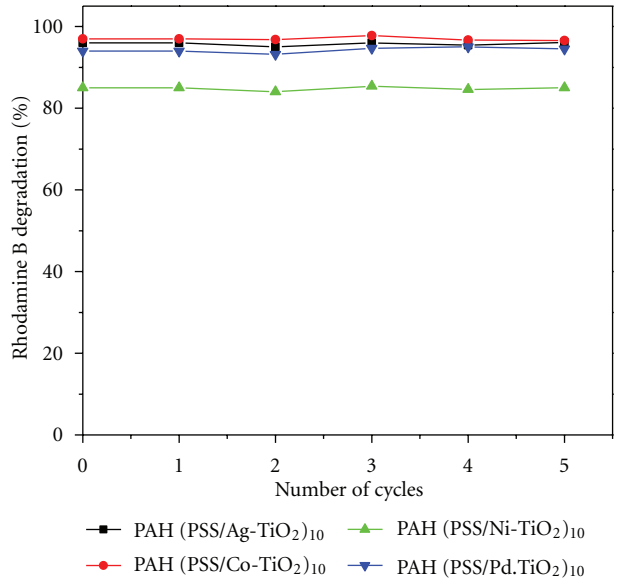

FIGURE 8: Catalyst reusability studies by the m-TiO_2 LbL assembled thin films.

obtained show that the LbL synthesised thin films did not lose their photocatalytic efficiencies even after the five cycles, that is, the photodegradation results of Rhodamine B were still reproducible even after the five cycles. The LbL self-assembled thin films therefore exhibited film stability. This is important because this observation suggests that the LbL assembled m-TiO_2 thin films could be potentially used in continuous water treatment systems. In addition, the reusability of the thin films means could result in a reduction in the cost of water treatment if m-TiO_2 thin films were to be utilised and if scaling up would still be as efficient and economically viable.

4. Conclusions

The m-TiO_2 LbL assembled thin films (PAH(PSS/m-TiO_2)$_n$) were successfully synthesised, and there was a linear increase in thickness as the number of multilayer deposition increased. These thin films exhibited high photodegradation efficiencies (up to 95%) of Rhodamine B under visible-light illumination. Although the illumination time was longer than when the suspension form is used, this can be overcome by increasing the number of thin film multilayers

to cause an increase in the rate of photocatalytic degradation of Rhodamine B. Catalyst reusability studies revealed that the LbL synthesised thin films were highly stable as they could maintain the equivalent photodegradation efficiencies for the five cycles that were tested. The high stability, reusability, and visible-light illumination of the m-TiO_2 make the LbL assembled m-TiO_2 thin films a potentially viable technique for application in water treatment processes where solar energy can be used as the source of energy for the illumination of photodegradation of pollutants in the presence of titania nanocatalysts.

Acknowledgments

The authors are grateful to the University of Johannesburg for financial support and the Indian Institute of Science, Bangalore, for providing the infrastructure to carry out most of this research work.

References

[1] D. N. Priya, J. M. Modak, and A. M. Raichur, "LbL fabricated poly(styrene sulfonate)/TiO_2 multilayer thin films for environmental applications," *ACS Applied Materials & Interfaces*, vol. 1, no. 1, pp. 2684–2693, 2009.

[2] R. S. Sonawane and M. K. Dongare, "Sol-gel synthesis of Au/TiO_2 thin films for photocatalytic degradation of phenol in sunlight," *Journal of Molecular Catalysis A*, vol. 243, no. 1, pp. 68–76, 2006.

[3] Z. He, C. Sun, S. Yang, Y. Ding, H. He, and Z. Wang, "Photocatalytic degradation of rhodamine B by Bi_2WO_6 with electron accepting agent under microwave irradiation: mechanism and pathway," *Journal of Hazardous Materials*, vol. 162, no. 2-3, pp. 1477–1486, 2009.

[4] A. Murakami, T. Yamaguchi, S. I. Hirano, and K. Kikuta, "Synthesis of porous titania thin films using carbonatation reaction and its hydrophilic property," *Thin Solid Films*, vol. 516, no. 12, pp. 3888–3892, 2008.

[5] L. Ge, M. Xu, and H. Fang, "Synthesis and characterization of the Pd/$InVO_4$–TiO_2 co-doped thin films with visible light photocatalytic activities," *Applied Surface Science*, vol. 253, no. 4, pp. 2257–2263, 2006.

[6] F. Ren, K. He, Y. Ling, and J. Feng, "Novel fabrication of net-like and flake-like Fe doped TiO_2 thin films," *Applied Surface Science*, vol. 257, pp. 9621–9625, 2011.

[7] B. Zhao and Y. Chen, "Ag/TiO_2 sol prepared by a sol-gel method and its photocatalytic activity," *Journal of Physics and Chemistry of Solids*, vol. 72, pp. 1312–1318, 2011.

[8] M. A. Nawi, A. H. Jawad, S. Sabar, and W. S. W. Ngah, "Immobilized bilayer TiO_2/chitosan system for the removal of phenol under irradiation by a 45 watt compact fluorescent lamp," *Desalination*, vol. 280, pp. 288–296, 2011.

[9] G. A. Battiston, R. Gerbasi, M. Porchia, and A. Marigo, "Influence of substrate on structural properties of TiO_2 thin films obtained via MOCVD," *Thin Solid Films*, vol. 239, no. 2, pp. 186–191, 1994.

[10] X. Hou, X. Wu, and A. Liu, "Studies on photocatalytic activity of Ag/TiO_2 films," *Frontiers of Chemistry in China*, vol. 1, no. 4, pp. 402–407, 2006.

[11] M. C. Kao, H. Z. Chen, S. L. Young, C. Y. Kung, C. C. Lin, and Z. Y. Hong, "Microstructure and optical properties of tantalum modified TiO_2 thin films prepared by the sol-gel process," *Journal of Superconductivity and Novel Magnetism*, vol. 23, no. 5, pp. 843–845, 2010.

[12] P. Romero-Gómez, V. Rico, J. P. Espinós, A. R. González-Elipe, R. G. Palgrave, and R. G. Egdell, "Nitridation of nanocrystalline TiO_2 thin films by treatment with ammonia," *Thin Solid Films*, vol. 519, no. 11, pp. 3587–3595, 2011.

[13] P. Wang, T. Zhou, R. Wang, and T. T. Lim, "Carbon-sensitized and nitrogen-doped TiO_2 for photocatalytic degradation of sulfanilamide under visible-light irradiation," *Water Research*, vol. 45, pp. 5015–5026, 2011.

[14] A. Bai, W. Liang, G. Zheng, and J. Xue, "Preparation and enhanced daylight-induced photo-catalytic activity of transparent C-Doped TiO_2 thin films," *Journal Wuhan University of Technology, Materials Science Edition*, vol. 25, no. 5, pp. 738–742, 2010.

[15] J. Yu, J. Xiong, B. Cheng, and S. Liu, "Fabrication and characterization of Ag-TiO_2 multiphase nanocomposite thin films with enhanced photocatalytic activity," *Applied Catalysis B*, vol. 60, no. 3-4, pp. 211–221, 2005.

[16] J. Yu, G. Dai, and B. Huang, "Fabrication and characterization of visible-light-driven plasmonic photocatalyst Ag/AgCl/TiO_2 nanotube arrays," *Journal of Physical Chemistry C*, vol. 113, no. 37, pp. 16394–16401, 2009.

[17] W. Q. Fang, J. Z. Zhou, J. Liu et al., "Hierarchical structures of single-crystalline anatase TiO_2 nanosheets dominated by 001 facets," *Chemistry*, vol. 17, no. 5, pp. 1423–1427, 2011.

[18] Q. Xiang, J. Yu, and M. Jaroniec, "Tunable photocatalytic selectivity of TiO_2 films consisted of flower-like microspheres with exposed 001 facets," *Chemical Communications*, vol. 47, no. 15, pp. 4532–4534, 2011.

[19] N. S. Begum, H. M. F. Ahmed, and K. R. Gunashekar, "Effects of Ni doping on photocatalytic activity of TiO_2 thin films prepared by liquid phase deposition technique," *Bulletin of Materials Science*, vol. 31, no. 5, pp. 747–751, 2008.

[20] W. Weng, M. Ma, P. Du et al., "Superhydrophilic Fe doped titanium dioxide thin films prepared by a spray pyrolysis deposition," *Surface and Coatings Technology*, vol. 198, no. 1–3, pp. 340–344, 2005.

[21] F. Meng, X. Song, and Z. Sun, "Photocatalytic activity of TiO_2 thin films deposited by RF magnetron sputtering," *Vacuum*, vol. 83, no. 9, pp. 1147–1151, 2009.

[22] Y. Cao, H. Tan, T. Shi, T. Shi, T. Tang, and J. Li, "Preparation of Ag-doped TiO_2 nanoparticles for photocatalytic degradation of acetamiprid in water," *Journal of Chemical Technology and Biotechnology*, vol. 83, no. 4, pp. 546–552, 2008.

[23] P. Bouras, E. Stathatos, and P. Lianos, "Pure versus metal-ion-doped nanocrystalline titania for photocatalysis," *Applied Catalysis B*, vol. 73, no. 1-2, pp. 51–59, 2007.

[24] E. Bae and W. Choi, "Highly enhanced photoreductive degradation of perchlorinated compounds on dye-sensitized metal/TiO_2 under visible light," *Environmental Science and Technology*, vol. 37, no. 1, pp. 147–152, 2003.

[25] T. Umebayashi, T. Yamaki, H. Itoh, and K. Asai, "Analysis of electronic structures of 3d transition metal-doped TiO_2 based on band calculations," *Journal of Physics and Chemistry of Solids*, vol. 63, no. 10, pp. 1909–1920, 2002.

[26] M. Stir, R. Nicula, and E. Burkel, "Pressure-temperature phase diagrams of pure and Ag-doped nanocrystalline TiO_2 photocatalysts," *Journal of the European Ceramic Society*, vol. 26, no. 9, pp. 1547–1553, 2006.

[27] A. Bhattacharyya, S. Kawi, and M. B. Ray, "Photocatalytic degradation of orange II by TiO_2 catalysts supported on adsorbents," *Catalysis Today*, vol. 98, no. 3, pp. 431–439, 2004.

[28] J. Yu, J. C. Yu, B. Cheng, and X. Zhao, "Photocatalytic activity and characterization of the sol-gel derived Pb-doped TiO_2 thin films," *Journal of Sol-Gel Science and Technology*, vol. 24, no. 1, pp. 39–48, 2002.

[29] A. López, D. Acosta, A. I. Martinez, and J. Santiago, "Nanostructured low crystallized titanium dioxide thin films with good photocatalytic activity," *Powder Technology*, vol. 202, no. 1–3, pp. 111–117, 2010.

[30] C. Zhang, R. Chen, J. Zhou, J. Cheng, and Q. Xia, "Synthesis of TiO_2 films on glass slides by the sol-gel method and their photocatalytic activity," *Rare Metals*, vol. 28, no. 4, pp. 378–384, 2009.

[31] X. S. Zhou, L. J. Li, Y. H. Lin, and C. W. Nan, "Characterization and properties of anatase TiO_2 film prepared via colloidal sol method under low temperature," *Journal of Electroceramics*, vol. 21, no. 1–4, pp. 795–797, 2008.

[32] Z. He, Z. Yu, H. Miao, G. Tan, and Y. Liu, "Preparation of TiO_2 thin film by the LPD method on functionalized organic self-assembled monolayers," *Science in China, Series E*, vol. 52, no. 1, pp. 137–140, 2009.

[33] J. Yu, X. Zhao, and Q. Zhao, "Effect of film thickness on the grain size and photocatalytic activity of the sol-gel derived nanometer TiO_2 thin films," *Journal of Materials Science Letters*, vol. 19, no. 12, pp. 1015–1017, 2000.

[34] A. Nakaruk and C. C. Sorrell, "Conceptual model for spray pyrolysis mechanism: fabrication and annealing of titania thin films," *Journal of Coatings Technology Research*, vol. 7, no. 5, pp. 665–676, 2010.

[35] D. Dumitriu, A. R. Bally, C. Ballif et al., "Photocatalytic degradation of phenol by TiO_2 thin films prepared by sputtering," *Applied Catalysis B*, vol. 25, no. 2-3, pp. 83–92, 2000.

[36] S.-H. Nam, S.-J. Cho, C.-K. Jung et al., "Comparison of hydrophilic properties of TiO_2 thin films prepared by sol-gel method and reactive magnetron sputtering system," *Thin Solid Films*, vol. 519, pp. 6944–6950, 2011.

[37] M. Guglielmi, A. Martucci, E. Menegazzo et al., "Control of semiconductor particle size in sol-gel thin films," *Journal of Sol-Gel Science and Technology*, vol. 8, no. 1–3, pp. 1017–1021, 1997.

[38] J. G. Yu, H. G. Yu, B. Cheng, X. J. Zhao, J. C. Yu, and W. K. Ho, "The effect of calcination temperature on the surface microstructure and photocatalytic activity of TiO_2 thin films prepared by liquid phase deposition," *Journal of Physical Chemistry B*, vol. 107, no. 50, pp. 13871–13879, 2003.

[39] J. Yu and B. Wang, "Effect of calcination temperature on morphology and photoelectrochemical properties of anodized titanium dioxide nanotube arratys," *Applied Catalysis B*, vol. 94, pp. 295–302, 2010.

[40] T. Sasaki, Y. Ebina, T. Tanaka, M. Harada, M. Watanabe, and G. Decher, "Layer-by-layer assembly of titania nanosheet/polycation composite films," *Chemistry of Materials*, vol. 13, no. 12, pp. 4661–4667, 2001.

[41] G. Decher, J. D. Hong, and J. Schmitt, "Buildup of ultrathin multilayer films by a self-assembly process—III. Consecutively alternating adsorption of anionic and cationic polyelectrolytes on charged surfaces," *Thin Solid Films*, vol. 210-211, no. 2, pp. 831–835, 1992.

[42] Y. Guo, W. Geng, and J. Sun, "Layer-by-layer deposition of polyelectrolyte-polyelectrolyte complexes for multilayer film fabrication," *Langmuir*, vol. 25, no. 2, pp. 1004–1010, 2009.

[43] M. E. Mahmoud, S. S. Haggag, and T. M. Abdel-Fattah, "Surface layer-by-layer chemical deposition reaction for thin film formation of nano-sized metal 8-hydroxyquinolate complexes," *Polyhedron*, vol. 28, no. 1, pp. 181–187, 2009.

[44] P. G. Su and Y. S. Chuang, "Flexible H_2 sensors fabricated by layer-by-layer self-assembly thin film of multi-walled carbon nanotubes and modified in situ with Pd nanoparticles," *Sensors and Actuators B*, vol. 145, no. 1, pp. 521–526, 2010.

[45] G. B. Sukhorukov, E. Donath, H. Lichtenfeld et al., "Layer-by-layer self assembly of polyelectrolytes on colloidal particles," *Colloids and Surfaces A*, vol. 137, no. 1–3, pp. 253–266, 1998.

[46] M. Yin, J. Qian, Q. An, Q. Zhao, Z. Gui, and J. Li, "Polyelectrolyte layer-by-layer self-assembly at vibration condition and the pervaporation performance of assembly multilayer films in dehydration of isopropanol," *Journal of Membrane Science*, vol. 358, no. 1-2, pp. 43–50, 2010.

[47] J. A. He, R. Mosurkal, L. A. Samuelson, L. Li, and J. Kumar, "Dye-sensitized solar cell fabricated by electrostatic layer-by-layer assembly of amphoteric TiO_2 nanoparticles," *Langmuir*, vol. 19, no. 6, pp. 2169–2174, 2003.

[48] X. Yang, X. Han, and Y. Zhu, "(PAH/PSS)5 microcapsules templated on silica core: encapsulation of anticancer drug DOX and controlled release study," *Colloids and Surfaces A*, vol. 264, no. 1–3, pp. 49–54, 2005.

[49] M. M. De Villiers, D. P. Otto, S. J. Strydom, and Y. M. Lvov, "Introduction to nanocoatings produced by layer-by-layer (LbL) self-assembly," *Advanced Drug Delivery Reviews*, vol. 63, no. 9, pp. 701–715, 2011.

[50] K. Murugan, T. N. Rao, G. V. N. Rao, A. S. Gandhi, and B. S. Murty, "Effect of dehydration rate on non-hydrolytic TiO_2 thin film processing: structure, optical and photocatalytic performance studies," *Materials Chemistry and Physics*, vol. 129, no. 3, pp. 810–815, 2011.

[51] S. Suárez, N. Arconada, Y. Castro et al., "Photocatalytic degradation of TCE in dry and wet air conditions with TiO_2 porous thin films," *Applied Catalysis B*, vol. 108-109, pp. 14–21, 2011.

[52] P. G. Su, W. C. Li, J. Y. Tseng, and C. J. Ho, "Fully transparent and flexible humidity sensors fabricated by layer-by-layer self-assembly of thin film of poly(2-acrylamido-2-methylpropane sulfonate) and its salt complex," *Sensors and Actuators B*, vol. 153, no. 1, pp. 29–36, 2011.

[53] T. H. Kim and B. H. Sohn, "Photocatalytic thin films containing TiO_2 nanoparticles by the layer-by-layer self-assembling method," *Applied Surface Science*, vol. 201, no. 1-4, pp. 109–114, 2002.

[54] C. Pan, L. Dong, L. Q. Ge, J. Wang, and Z. Z. Gu, "Highly active TiO_2/polyelectrolytes hybrid multilayered hollow nanofibrous photocatalyst prepared from electrouspun fibers using electrostatic layer-by-layer technique," *Journal of Macromolecular Science Part B*, vol. 48, no. 1, pp. 92–105, 2009.

[55] T. S. Natarajan, M. Thomas, K. Natarajan, H. C. Bajaj, and R. J. Tayade, "Study on UV-LED/TiO_2 process for degradation of Rhodamine B dye," *Chemical Engineering Journal*, vol. 169, no. 1–3, pp. 126–134, 2011.

[56] M. Akarsu, M. Asiltürk, F. Sayilkan, N. Kiraz, E. Arpaç, and H. Sayilkan, "A novel approach to the hydrothermal synthesis of anatase titania nanoparticles and the photocatalytic degradation of Rhodamine B," *Turkish Journal of Chemistry*, vol. 30, no. 3, pp. 333–343, 2006.

[57] J. Zhu, J. Zhang, F. Chen, K. Iino, and M. Anpo, "High activity TiO_2 photocatalysts prepared by a modified sol-gel method: characterization and their photocatalytic activity for the degradation of XRG and X-GL," *Topics in Catalysis*, vol. 35, no. 3-4, pp. 261–268, 2005.

[58] Y. Ao, J. Xu, D. Fu, and C. Yuan, "Preparation of Ag-doped mesoporous titania and its enhanced photocatalytic activity under UV light irradiation," *Journal of Physics and Chemistry of Solids*, vol. 69, no. 11, pp. 2660–2664, 2008.

[59] J. A. Navio, G. Colon, M. Macias, C. Real, and M. I. Litter, "Iron-doped titania semiconductor powders prepared by a sol-gel method—part I: synthesis and characterization," *Applied Catalysis A*, vol. 177, pp. 111–120, 1999.

[60] K. Katagiri, T. Suzuki, H. Muto, M. Sakai, and A. Matsuda, "Low temperature crystallization of TiO_2 in layer-by-layer assembled thin films formed from water-soluble Ti-complex and polycations," *Colloids and Surfaces A*, vol. 321, no. 1–3, pp. 233–237, 2008.

[61] G. Decher, B. Lehr, K. Lowack, Y. Lvov, and J. Schmitt, "New nanocomposite films for biosensors: layer-by-layer adsorbed films of polyelectrolytes, proteins or DNA," *Biosensors and Bioelectronics*, vol. 9, no. 9-10, pp. 677–684, 1994.

[62] P. Ding, F. M. Liu, X. A. Yang, and J. Q. Li, "Characterization of structure and distortion in the manganese ions implanted TiO_2 thin films," *Nuclear Instruments and Methods in Physics Research Section B*, vol. 267, no. 18, pp. 3109–3113, 2009.

[63] J. H. Kim, S. Fujita, and S. Shiratori, "Fabrication and characterization of TiO_2 thin film prepared by a layer-by-layer self-assembly method," *Thin Solid Films*, vol. 499, no. 1-2, pp. 83–89, 2006.

[64] A. Izquierdo, S. S. Ono, J. C. Voegel, P. Schaaf, and G. Decher, "Dipping versus spraying: exploring the deposition conditions for speeding up layer-by-layer assembly," *Langmuir*, vol. 21, no. 16, pp. 7558–7567, 2005.